Vol 464|15 April 2010|doi:10.1038/nature08943

ARTICLES

Molecular basis of infrared detection by snakes

Elena O. Gracheva[1]*, Nicholas T. Ingolia[2,3,4]*, Yvonne M. Kelly[1], Julio F. Cordero-Morales[1], Gunther Hollopeter[1]†, Alexander T. Chesler[1], Elda E. Sánchez[5], John C. Perez[5], Jonathan S. Weissman[2,3,4] & David Julius[1,2]

Snakes possess a unique sensory system for detecting infrared radiation, enabling them to generate a 'thermal image' of predators or prey. Infrared signals are initially received by the pit organ, a highly specialized facial structure that is innervated by nerve fibres of the somatosensory system. How this organ detects and transduces infrared signals into nerve impulses is not known. Here we use an unbiased transcriptional profiling approach to identify TRPA1 channels as infrared receptors on sensory nerve fibres that innervate the pit organ. TRPA1 orthologues from pit-bearing snakes (vipers, pythons and boas) are the most heat-sensitive vertebrate ion channels thus far identified, consistent with their role as primary transducers of infrared stimuli. Thus, snakes detect infrared signals through a mechanism involving radiant heating of the pit organ, rather than photochemical transduction. These findings illustrate the broad evolutionary tuning of transient receptor potential (TRP) channels as thermosensors in the vertebrate nervous system.

Venomous pit vipers detect warm-blooded prey through their ability to sense infrared (750 nm–1 mm wavelength) radiation. Superimposition of thermal and visual images within the snake's brain enables it to track animals with great precision and speed. Biophysical studies suggest that this system is exquisitely sensitive, such that vipers can detect prey at distances of up to 1 m. Infrared sensation may also be important for predator avoidance and thermoregulatory behaviour[1–3].

The western diamondback rattlesnake (*Crotalus atrox*) is a highly evolved viper whose ability to detect infrared radiation is unmatched by other snakes. Infrared detection is mediated by specialized loreal pit organs located between the eye and nostril on either side of the viper's face (Fig. 1a)[4]. Suspended within each of these hollow chambers is a thin membrane that serves as an infrared antenna (Fig. 1b). The membrane is rich in mitochondria, highly vascularized, and densely innervated by primary afferent nerve fibres from the trigeminal branch of the somatosensory system (Supplementary Fig. 1a)[5–8]. These fibres convey infrared signals from the pit organ to the optic tectum of the brain, where they converge with input from other sensory modalities[9–11]. Some members of the non-venomous *Pythonidae* and *Boidae* families (pythons and boas, respectively) also detect infrared radiation, albeit with 5–10-fold lower sensitivity than *Crotalinae* vipers[3,12,13]. Pythons and boas possess labial pit organs, which are distributed over the snout and lack the complex architecture seen in loreal pits of vipers (Supplementary Fig. 1b). Nonetheless, they are similarly vascularized and innervated by trigeminal fibres, but at lower density[5,14–16]. Thus, relative sensitivities of these snake species to infrared radiation probably reflect molecular and anatomical differences of this specialized sensory system. Although the role of the pit organ as an infrared sensor is well established, fundamental questions remain about its mechanism of stimulus detection. For example, it is unclear whether the membrane itself contains the infrared sensor, or whether the sensor is expressed by the closely apposed nerve fibres. Moreover, the molecular identity of the infrared sensor is unknown, and thus how its intrinsic biophysical characteristics account for the physiological properties of the pit organ has yet to

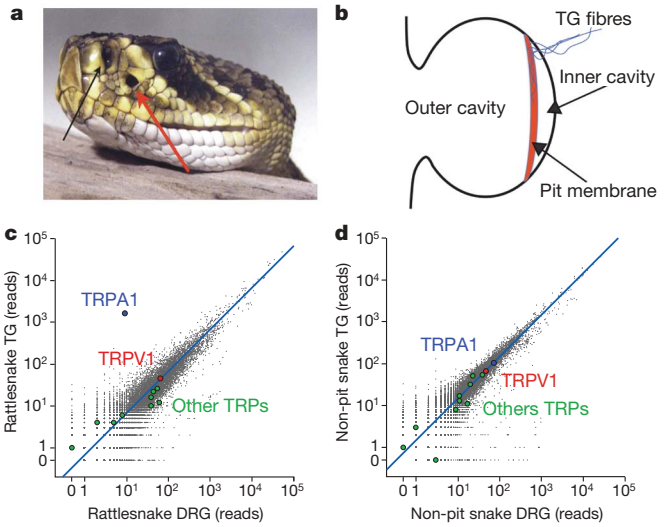

Figure 1 | Anatomy of the pit organ and comparison of gene expression in snake sensory ganglia. a, Rattlesnake head showing location of nostril and loreal pit organ (black and red arrows, respectively) (from Wikimedia Commons). **b**, Schematic of pit organ structure showing innervation of pit membrane suspended within hollow cavity. **c**, **d**, Number of mRNA-Seq reads from snake ganglia that align to the chicken proteome. TRPA1 and TRPV1 are highlighted, as are other TRP channels. Blue line indicates expected number of sequencing reads for genes with similar expression levels in the two samples based on the total number of aligned reads from each. Signals <20 reads are within statistical noise and therefore scored as non-expressed sequences. Rattlesnake refers to *C. atrox* (**c**), non-pit refers to a combination of Texas rat (*Elaphe obsoleta lindheimeri*) and western coachwhip (*Masticophis flagellum testaceus*) snakes (**d**).

[1]Department of Physiology, [2]Department of Cellular and Molecular Pharmacology, [3]Howard Hughes Medical Institute, [4]California Institute for Quantitative Biosciences, University of California, San Francisco, California 94158-2517, USA. [5]Natural Toxins Research Center, Texas A&M University- Kingsville, Texas 78363, USA. †Present address: Department of Biology, University of Utah, 257 South 1400 East, Salt Lake City, Utah 84112-0840, USA.
*These authors contributed equally to this work.

be established. Also at issue is whether *Crotalinae*, *Pythonidae* and *Boidae* snakes use similar molecular strategies for sensing infrared radiation.

In principle, an infrared receptor could detect photons directly, similar to photochemical activation of opsins in the eye, or indirectly through heating of tissue within the pit, leading to activation of a thermoreceptor[1]. Because the pit receives direct input from the somatosensory, rather than the visual system[9], it seems likely that infrared signals are detected through a thermotransduction, rather than a phototransduction mechanism. Consistent with this, heat-activated membrane currents from rattlesnake trigeminal neurons have been described, although their functional properties have not been extensively characterized[6,17].

Snakes, particularly pit vipers, are inconvenient subjects for physiological and behavioural studies. They are also genetically intractable organisms for which annotated genomic information is scarce, limiting molecular studies of infrared detection. We therefore used transcriptome profiling to identify pit-enriched sensory transducers, yielding the snake orthologue of the 'wasabi receptor', TRPA1, as a candidate infrared detector. This channel is highly enriched in trigeminal neurons that innervate the pit and, when heterologously expressed, exhibits robust heat-sensitivity. Thus, TRPA1 has been evolutionarily selected to function as a specialized and highly sensitive heat receptor in the pit, whereas in mammals it functions primarily as a detector of chemical irritants and inflammatory agents[18]. Our results demonstrate that the pit membrane serves as a passive antenna for radiant heat, transducing thermal energy to heat-sensitive channels on embedded nerve fibres.

Exploiting specialization of pit vipers

In most sensory systems, specialized receptor cells detect relevant stimuli and transmit signals to adjacent nerve fibres. In the somatosensory system, however, bare nerve endings are themselves detectors of thermal, mechanical or chemical stimuli[19]. Indeed, trigeminal ganglia (TG) of pit-bearing snakes are unusually large compared to those of mammals, and send a thick bundle of afferents directly to the pit on the ipsilateral side of the face (Supplementary Fig. 1a)[20,21]. We therefore reasoned that snake TG should express proteins dedicated to pit function, and that such proteins should be less abundant in dorsal root ganglia (DRG), which provide somatosensory input to the trunk. Because mammalian TG and DRG gene expression profiles are more-or-less equivalent[22,23], marked differences in snakes should reflect functional specialization associated with infrared detection. Remarkably, a pair-wise comparison of transcriptomes from rattlesnake TG versus DRG highlighted a single gene encoding an orthologue of the TRPA1 ion channel (Fig. 1c). Whereas other members of the TRP channel family (for example, the capsaicin- and heat-activated receptor, TRPV1) showed equivalent expression in these ganglia, TRPA1 was enriched 400-fold in TG.

If TRPA1 is of unique functional importance to infrared sensing, then snakes lacking pit organs (non-pit species) should not show a disparity in TRPA1 expression between TG and DRG. Indeed, transcriptomes from two non-pit species—Texas rat and western coachwhip snakes—showed no obvious outliers for either ganglion (Fig. 1d). Consistent with this, transcriptome comparison from TG of rattlesnake versus non-pit snakes again identified *TRPA1* as the only differentially expressed gene (Supplementary Fig. 1c). In stark contrast to non-pit snakes and other vertebrates, *TRPA1* transcripts were absent from rattlesnake DRG (Supplementary Fig. 1d), further supporting a specific role for this channel in TG/pit function. Lastly, we did not detect opsin-like sequences in TG of any snake species examined.

Unique expression of TRPA1 in viper TG

Vertebrate somatosensory ganglia contain anatomically and functionally diverse neuronal subpopulations[24]. In general, neurons having the largest soma diameters are involved in the detection of innocuous sensations, such as light touch, whereas small to medium diameter neurons constitute most nociceptors that detect noxious stimuli. In mammals, TRPA1 is expressed by ~25% of all somatosensory neurons, preferentially nociceptors that also express TRPV1 (refs 25, 26). We observed a very different anatomical profile in rattlesnakes, where most TG neurons were medium-to-large diameter, 59.9 ± 9.7% (mean ± s.d.) of which expressed TRPA1 (Fig. 2a, b) (also see later). Consistent with our transcriptome analysis, no TRPA1 signal was observed in rattlesnake DRG (Fig. 2a, c). We also examined the distribution of TRPV1, which in rodent TG or DRG is expressed by 40–60% of neurons, predominantly nociceptors[26,27]. In rattlesnake TG or DRG, TRPV1 was expressed by only 13 ± 4.1% or 14.5 ± 5.7% of neurons, respectively, most with small diameters (Fig. 2a, c). Thus, pit viper TG is unique among vertebrates, reflecting adaptation for infrared detection.

Snake TRPA1 is a heat-activated channel

Mammalian TRPA1 is activated by allyl isothiocyanate (AITC), the pungent agent from wasabi and other mustard plants[25,28]. AITC and other electrophilic irritants gate the channel through an unusual mechanism involving covalent modification of cysteine residues within the cytoplasmic amino terminus[29,30]. Rattlesnake and rat snake TRPA1 show 81% identity with one another and 63% identity with human TRPA1, and contain three conserved N-terminal cysteines required for activation by electrophiles (Supplementary Fig. 2). Indeed, when expressed in HEK293 cells, TRPA1 from either snake species responded to AITC, demonstrating functionality of the cloned channels (Fig. 3a).

If TRPA1 is important for infrared sensing, then it should respond to thermal stimuli in a temperature range consistent with sensitivity

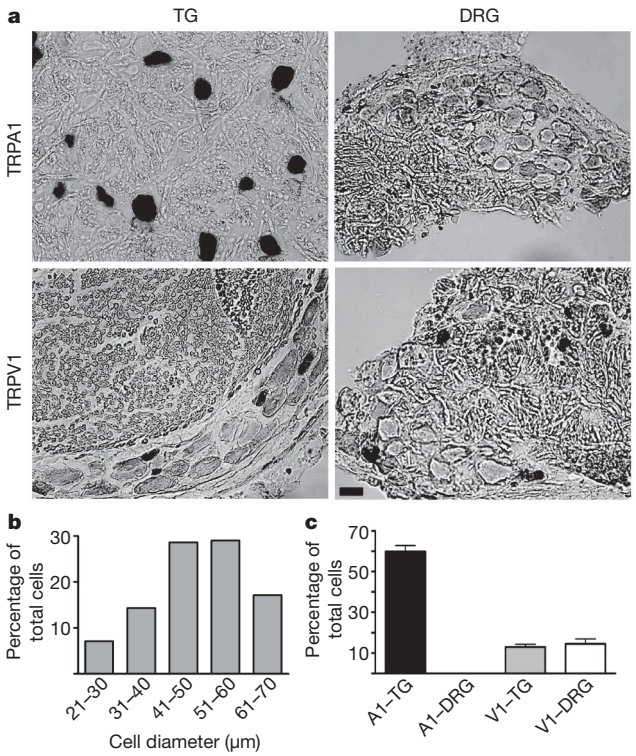

Figure 2 | Expression of TRPA1 and TRPV1 in rattlesnake sensory ganglia. **a**, *In situ* hybridization showing expression of TRPA1 or TRPV1 in tissue sections from rattlesnake TG or DRG, as indicated. Scale bar, 20 μm. **b**, Quantification of neuronal cell size (diameter) determined from histological sections of rattlesnake TG ($n = 70$ cells from five independent sections). **c**, Quantitative analysis of cells within TG or DRG that express *TRPA1* or *TRPV1* transcripts (mean ± s.d.; $n = 448$ neurons from 11 independent sections for *TRPA1*, and $n = 151$ neurons from 5 independent sections for *TRPV1*).

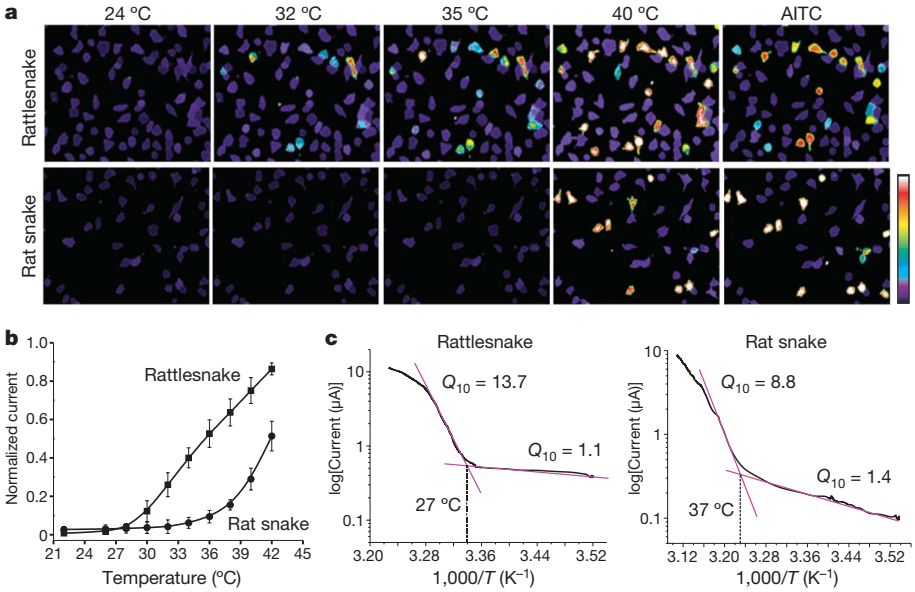

Figure 3 | Functional analysis of snake TRPA1 channels. a, HEK293 cells expressing cloned rattlesnake or rat snake TRPA1 channels were analysed for heat or mustard oil (200 μM AITC; 24 °C)-evoked responses using calcium imaging; colour bar indicates relative change in fluorescence ratio, with purple and white denoting the lowest and highest cytoplasmic calcium, respectively ($n \geq 105$ cells per channel). **b**, Relative heat response profiles of rattlesnake and rat snake channels expressed in oocytes (response at each temperature was normalized to the maximal response at 45 °C; holding potential (V_H) = −80 mV; $n \geq 6$). Data show mean ± s.d. **c**, Arrhenius plots show thermal thresholds and Q_{10} values for baseline and evoked responses of rattlesnake (left) and rat snake (right) TRPA1 channels, as indicated (temperature ramp of 1 °C s^{-1}).

of the pit, which detects changes in ambient temperature above ~30 °C (ref 17). Indeed, rattlesnake TRPA1 was inactive at room temperature, but robustly activated above 28.0 ± 2.5 °C (Fig. 3a and Supplementary Fig. 3a). Interestingly, rat snake TRPA1 was also heat-sensitive, albeit with a substantially higher threshold of 36.3 ± 0.6 °C. To assess thermal response profiles in greater detail, we measured heat-evoked membrane currents in voltage-clamped *Xenopus* oocytes expressing snake channels. Consistent with calcium imaging data, rattlesnake TRPA1 showed extremely robust and steep responses to heat with a threshold of 27.6 ± 0.9 °C (Q_{10} = 13.7), whereas the rat snake channel responded with a higher threshold of 37.2 ± 0.7 °C (Q_{10} = 8.8) (Fig. 3b, c and Supplementary Fig. 3b). Thus, although the rat snake channel is heat-sensitive, its thermal response properties make it less well suited to act as an infrared sensor than the pit viper channel. Instead, TRPA1, in conjunction with TRPV1, may contribute to cutaneous and somatic thermosensation in non-pit snakes, consistent with the higher activation thresholds of rat snake versus rattlesnake TRPA1. The rattlesnake channel did not respond to cold (12 °C) (not shown).

TRPA1 channels have been characterized from several vertebrate species, including fish[31], all of which are activated by AITC, but not heat (Supplementary Fig. 4). TRPA1-like channels are also found in invertebrate organisms, including *Drosophila melanogaster*, whose genome contains three *TRPA1* orthologues. One of these (d*TrpA1*) is heat-sensitive[32,33], and in our experimental conditions shows a thermal threshold of 33.7 ± 1.0 °C (Supplementary Fig. 5). Relative to rat TRPA1, which responds to AITC with a half-maximum effective concentration (EC_{50}) of 11 μM, the rattlesnake and rat snake orthologues are less sensitive, showing robust responses at concentrations ≥500 μM and with significantly slower activation. The relative sensitivities of these channels to heat versus AITC are clearly shown by comparing current–voltage profiles (Supplementary Fig. 3b). This inverse relationship between heat- and AITC-sensitivity probably underscores the relative contribution of TRPA1 to thermo- versus chemosensation in different organisms. Taken together, our bioinformatics, and anatomical and functional results strongly indicate that TRPA1 serves as an infrared detector in the pit viper.

Ancient snakes use TRPA1 to sense infrared radiation

Ancient (pythons and boas) and modern (pit vipers) snakes are separated by a long evolutionary distance (>30 million years) and show substantial differences in pit architecture and sensitivity[34,35]. We therefore asked whether they use the same molecule to detect heat. In sensory ganglia of royal python (*Python regius*) and amazon tree boa (*Corallus hortulanus*), *TRPA1*, again, stood out as the major differentially expressed transcript, being 65- and 170-fold more abundant in TG than DRG for pythons and boas, respectively (Fig. 4a, b). Moreover, comparison of transcript ratios from rattlesnake and python showed that TRPA1 stands alone as a highly TG-specific molecule (Supplementary Fig. 6a). In contrast to pit vipers, TRPA1 was expressed in DRG of python and boa, but only at relatively modest levels, comparable to that of other TRP channels. Surprisingly, *TRPV1* transcripts were not observed above background levels in pythons (Fig. 4a), suggesting that TRPA1 or another heat-sensitive channel underlies somatic thermosensation in this species.

Dendrogram analysis of snake TRPA1 channels shows that they constitute a closely related subfamily of heat-sensitive orthologues (Fig. 4c). Moreover, the position of boa and python sequences supports the hypothesis that these species represent an evolutionarily ancient branch of snakes that is independent of modern snakes such as pit vipers or rat snakes.

Expression of cloned python and boa TRPA1 in oocytes showed that both are heat-activated channels with modest sensitivity to AITC (Fig. 4d and Supplementary Fig. 6b, c). Interestingly, we found that python and boa channels exhibited a slightly higher thermal threshold compared to rattlesnake TRPA1 (32.7 ± 1.3 °C and 29.6 ± 0.7 °C, respectively, versus 27.6 ± 0.9 °C for rattlesnake), consistent with differential sensitivity of these snakes to infrared radiation. As in the case of the rattlesnake channel, python and boa TRPA1 were substantially more sensitive to heat than chemical agonists, as evidenced by relatively small responses to AITC (Supplementary Fig. 6b, c).

Endogenous TRPA1 subserves infrared detection

To assess the contribution of TRPA1 to neuronal heat sensitivity, we chose pythons as a convenient (that is, non-venomous) pit-bearing

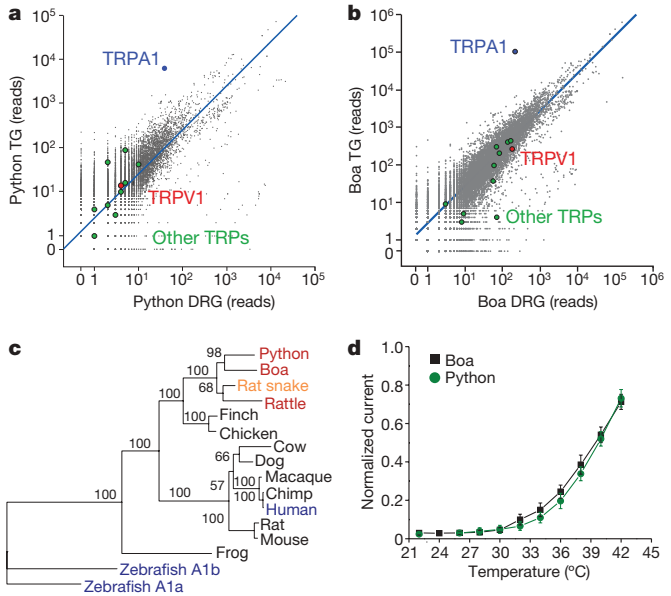

Figure 4 | Analysis of TRPA1 from python and boa. **a**, **b**, Transcriptome profiling of ancient snakes. Number of mRNA-Seq reads from python (**a**) and boa (**b**) ganglia that align to the chicken proteome, as described in Fig. 1. **c**, Phylogenetic tree of TRPA1 channel protein sequences with bootstrap values from 100 trials. Red denotes heat-sensitive channels with a lower thermal threshold than rat snake (orange). Blue indicates non-heat-sensitive channels according to this study. **d**, Relative heat response profiles for python and boa TRPA1 as measured in oocytes (recorded and normalized as described in Fig. 3b). Data show mean ± s.d.

species for functional studies. Anatomically, python TG resemble those of rattlesnakes, consisting primarily of large and medium diameter neurons, most of which (73.1 ± 7.8%) express TRPA1 (Fig. 5a and Supplementary Fig. 7a, b). Consistent with this, most (78.2 ± 14.0%) neurons from python TG were heat-sensitive and exhibited a threshold of 28.0 ± 2.2 °C (Fig. 5b). Moreover, all heat-sensitive neurons responded to 500 μM AITC (not shown), confirming expression of functional TRPA1 channels in these cells. No capsaicin-sensitive neurons were observed in python TG cultures, consistent with our bioinformatics profile showing lack of TRPV1 in these ganglia.

TG from control rat snake more closely resembled those of mammals in the relative proportion of small, medium and large diameter neurons. Compared to pit-bearing species, TRPA1 was expressed by a restricted cohort (13.3 ± 5.7%) of rat snake TG neurons that included mostly small and medium diameter cells (Fig. 5a and Supplementary Fig. 7a). Unlike pythons, rat snake TG contained a considerable proportion (27.3 ± 4.4%) of TRPV1-positive neurons (Supplementary Fig. 7a), suggesting that both TRPA1 and TRPV1 contribute to heat sensation in this species. Neurons from rat snake TG also showed a lower prevalence (~20%) of heat- and AITC-sensitivity compared to pythons, and responders were confined to the medium/small diameter subpopulation (Supplementary Fig. 7b). Notably, rat snake neurons responded at higher temperatures, binning into two distinct populations with thresholds of 36.2 ± 1.8 °C and 38.7 ± 1.4 °C ($P < 0.025$), the former being AITC-sensitive and the latter being capsaicin-sensitive (Fig. 5b and Supplementary Fig. 7c). Taken together, our results indicate that TRPA1 underlies infrared and somatic heat sensation in pit-bearing snakes, whereas TRPA1 and TRPV1 contribute to somatic thermosensation in rat

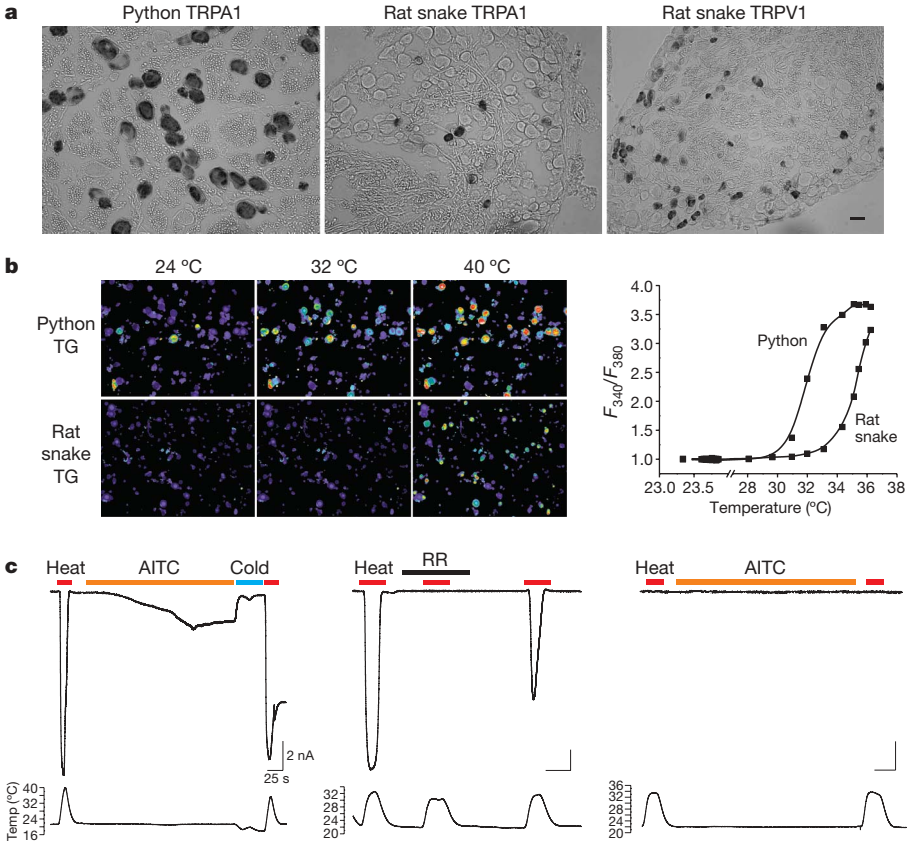

Figure 5 | Functional analysis of snake sensory neurons. **a**, Expression of TRPA1 or TRPV1 transcripts in python and rat snake TG. Scale bar, 40 μm. **b**, Thermal sensitivity of python and rat snake TG neurons as measured by calcium imaging. Temperature ramps (24 to 46 °C) were applied by continuous perfusion to assess thresholds (colour scale as in Fig. 3a). Corresponding temperature-response profiles are shown at the right ($n = 5$ and 26 neurons, respectively). Thresholds (28.0 ± 0.7 and 36.2 ± 0.6; $P < 0.0001$) were determined from an average of 43 and 89 neurons from python and rat snake, respectively (10 independent fields each). **c**, Patch-clamp recordings from python neurons showing robust heat- and AITC-evoked currents that were suppressed by cold (left) and blocked by ruthenium red (RR, 10 μM) (centre) ($n > 45$). A minority of neurons was insensitive to heat and AITC (right) ($n > 8$).

snakes. Furthermore, the functional properties and tissue distribution of rattlesnake TRPV1 (Supplementary Fig. 8 and Fig. 2a, c) make it a likely candidate for mediating somatic thermosensation in this species.

Finally, patch-clamp recording verified the presence of heat-sensitive membrane currents in snake neurons. Most python TG neurons showed enormous heat-evoked currents bearing the hallmarks of TRPA1 channels, including blockade by ruthenium red, inward rectification, and desensitization (Fig. 5c and Supplementary Fig. 7d). Like heterologously expressed python TRPA1, these responses were attenuated (~50%) by the mammalian TRPA1 antagonist HC-030031 (not shown). Consistent with our calcium imaging results, heat-sensitive python TG neurons also responded to AITC and showed a thermal threshold of 29.5 ± 1.7 °C. A more restricted population of medium diameter neurons were insensitive to heat or AITC (Fig. 5c), although they showed robust action potential firing after depolarization (not shown). In contrast with pythons, the activation threshold for heat-sensitive rat snake neurons was substantially higher (35.6 ± 1.2 °C) (Supplementary Fig. 7d).

Discussion

Four vertebrate families possess specialized sensory organs devoted to the detection of infrared radiation: pit viper, python, and boa families of snakes, as well as vampire bats[2,36]. Here we delineate the mechanism whereby three of these families sense infrared radiation, starting with the pit viper as the paragon of this unique sensory modality. We accomplished this by taking an unbiased transcriptome profiling approach in which minimal assumptions were made about the molecular specialization of the pit and associated neural structures. This represents a powerful, sensitive and quantitative version of the classic plus–minus screen for identifying organ-specific genes. We exploited this technology to address a problem vexed by a paucity of tissue and lack of genomic information.

In vertebrates, temperature sensation is mediated through activation of TRP channels that detect heat or cold[37]. In invertebrate organisms, such as flies (*Drosophila*), activation of TRP channels also contributes to temperature detection[32,33], whereas in worms (*Caenorhabditis elegans*), thermosensation is suggested to involve a phototransduction-like pathway involving activation of cyclic nucleotide-gated channels[38,39]. Our analysis suggests that the pit organ detects infrared radiation through a TRP channel-based process, rather than an opsin-like pathway, consistent with thermal, rather than photochemical signal transduction.

Identification of snake TRPA1 as an infrared sensor is interesting from an evolutionary perspective because previously identified vertebrate TRPA1 orthologues function primarily as detectors of chemical irritants[18], and possibly cold[40,41]. Thus, snake TRPA1 is functionally more like its invertebrate counterparts, despite their greater sequence diversity. Recent observations suggest that among TRP channels, TRPA1 orthologues show particularly rapid evolution in invertebrate species, where they display a range of heat sensitivities and contribute differentially to thermosensation[42,43]. Our findings indicate that this functional diversification extends to vertebrate channels, as well. Although the evolutionary relationship among snake species is a subject of continuing study and debate[34,44], our phylogenetic analysis indicates that ancient and modern snakes have independently adapted TRPA1 as an infrared sensor through convergent evolution. The cloned rattlesnake channel is the most heat-sensitive (that is, lowest thermal activation threshold and highest Q_{10}), in keeping with the greater infrared acuity of pit vipers compared to pythons or boas[3]. At the same time, differences in thermosensitivity among snake TRPA1 channels can differ by as little as 2 °C (for example, rattlesnake versus boa), suggesting that other cellular or anatomical factors contribute to physiological and behavioural differences in stimulus detection. Finally, the relative contributions of TRPA1 and other heat-sensitive channels (such as TRPV1) to somatic thermosensation probably differ among snake species, depending on thermal thresholds and expression patterns.

Sensory systems evolve rapidly to accommodate variations in environmental niche, such as those affecting climate and predator–prey relationships[45,46]. TRPA1 channels have undergone particularly fascinating evolutionary perturbation and selection to function as thermo- or chemoreceptors in organisms of very different lineage, indicative of their unique physiological plasticity throughout the animal kingdom. Thus, TRPA1 and other TRP channels provide new genetic and physiological markers with which to delineate evolutionary relationships among vertebrate and invertebrate species.

METHODS SUMMARY

Complementary DNA libraries were sequenced on Illumina Genome Analyser II and aligned to chicken RefSeq protein database. The unrooted phylogenetic tree was constructed from multiple sequence alignments using PhyML (version 3.0). Bootstrapping was performed with 100 trials. Adult snake tissue was fixed with paraformaldehyde for chromogenic *in situ* hybridization histochemistry. Rattlesnakes were provided by the Natural Toxins Research Center, Texas A&M University-Kingsville; boas, pythons and rat snakes were obtained from Glades Herp Farm. Animal husbandry and euthanasia procedures were approved by the University of California, San Francisco (UCSF) or University of Texas Institutional Animal Care and Use Committee. Cloned channels were transiently expressed in HEK293 cells and subjected to calcium imaging using Fura-2/AM ratiometric dye. Snake TG neurons were cultured as previously described[17]. Oocytes from *Xenopus laevis* were cultured, injected with 5 ng RNA, and analysed 2–5 days after injection by two-electrode voltage-clamp (TEVC) as described[47]. Membrane currents were recorded under the whole-cell patch-clamp configuration and thermal stimulation applied with a custom-made Peltier device (Reid-Dan Electronics). Temperature thresholds represent the point of intersection between linear fits to baseline and the steepest component of the Arrhenius profile, as described[48].

Full Methods and any associated references are available in the online version of the paper at www.nature.com/nature.

Received 23 September 2009; accepted 24 February 2010.
Published online 14 March; corrected 15 April 2010 (see full-text HTML version for details).

1. Bullock, T. H. & Cowles, R. B. Physiology of an infrared receptor: the facial pit of pit vipers. *Science* **115,** 541–543 (1952).
2. Campbell, A. L., Naik, R. R., Sowards, L. & Stone, M. O. Biological infrared imaging and sensing. *Micron* **33,** 211–225 (2002).
3. Ebert, J. *Infrared Sense in Snakes – Behavioural and Anatomical Examinations* (Crotalus atrox, Python regius, Corallus hortulanus). Dr rer. nat. thesis, Rheinische Friedrich Wilhelms Univ. Bonn (2007).
4. Barrett, R., Maderson, P. F. A. & Meszler, R. M. in *Biology of Reptilia* (ed. Parsons, T. S.) Ch. 4, 277–300 (Academic Press, 1970).
5. Ebert, J. & Schmitz, A. in *Herpetologia Bonnensis II* (eds Vences, M. Kohler, J., Ziegler T. & Bohme, W.) 215–217 (2006).
6. Terashima, S. & Liang, Y. F. Temperature neurons in the crotaline trigeminal ganglia. *J. Neurophysiol.* **66,** 623–634 (1991).
7. Amemiya, F., Ushiki, T., Goris, R. C., Atobe, Y. & Kusunoki, T. Ultrastructure of the crotaline snake infrared pit receptors: SEM confirmation of TEM findings. *Anat. Rec.* **246,** 135–146 (1996).
8. Bleichmar, H. & De Robertis, E. Submicroscopic morphology of the infrared receptor of pit vipers. *Z. Zellforsch. Mikrosk. Anat.* **56,** 748–761 (1962).
9. Hartline, P. H., Kass, L. & Loop, M. S. Merging of modalities in the optic tectum: infrared and visual integration in rattlesnakes. *Science* **199,** 1225–1229 (1978).
10. Newman, E. A. & Hartline, P. H. Integration of visual and infrared information in bimodal neurons in the rattlesnake optic tectum. *Science* **213,** 789–791 (1981).
11. Molenaar, G. J. The sensory trigeminal system of a snake in the possession of infrared receptors. II. The central projections of the trigeminal nerve. *J. Comp. Neurol.* **179,** 137–151 (1978).
12. de Cock Buning, T., Terashima, S. & Goris, R. C. Python pit organs analyzed as warm python pit organs analyzed as warm receptors. *Cell. Mol. Neurobiol.* **1,** 271–278 (1981).
13. Warren, J. W. & Proske, U. Infrared receptors in the facial pits of the Australian python Morelia spilotes. *Science* **159,** 439–441 (1968).
14. Kishida, R., Amemiya, F., Kusunoki, T. & Terashima, S. A new tectal afferent nucleus of the infrared sensory system in the medulla oblongata of Crotaline snakes. *Brain Res.* **195,** 271–279 (1980).
15. Kishida, R., de Cock Buning, T. & Dubbeldam, J. L. Primary vagal nerve projections to the lateral descending trigeminal nucleus in boidae (*Python molurus* and *Boa constrictor*). *Brain Res.* **263,** 132–136 (1983).
16. Noble, G. K. & Schmidt, A. The structure and function of facial and labial pits of snakes. *Proc. Am. Phil. Soc.* **77,** 263–288 (1937).

17. Pappas, T. C., Motamedi, M. & Christensen, B. N. Unique temperature-activated neurons from pit viper thermosensors. *Am. J. Physiol. Cell Physiol.* **287,** C1219–C1228 (2004).
18. Bautista, D. M. *et al.* TRPA1 mediates the inflammatory actions of environmental irritants and proalgesic agents. *Cell* **124,** 1269–1282 (2006).
19. Julius, D. & Basbaum, A. I. Molecular mechanisms of nociception. *Nature* **413,** 203–210 (2001).
20. Molenaar, G. J. An additional trigeminal system in certain snakes possessing infrared receptors. *Brain Res.* **78,** 340–344 (1974).
21. Schroeder, D. M. & Loop, M. S. Trigeminal projections in snakes possessing infrared sensitivity. *J. Comp. Neurol.* **169,** 1–13 (1976).
22. Eng, S. R., Dykes, I. M., Lanier, J., Fedtsova, N. & Turner, E. E. POU-domain factor Brn3a regulates both distinct and common programs of gene expression in the spinal and trigeminal sensory ganglia. *Neural Dev.* **2,** 3 (2007).
23. Su, A. I. *et al.* A gene atlas of the mouse and human protein-encoding transcriptomes. *Proc. Natl Acad. Sci. USA* **101,** 6062–6067 (2004).
24. Woolf, C. J. & Ma, Q. Nociceptors–noxious stimulus detectors. *Neuron* **55,** 353–364 (2007).
25. Jordt, S. E. *et al.* Mustard oils and cannabinoids excite sensory nerve fibres through the TRP channel ANKTM1. *Nature* **427,** 260–265 (2004).
26. Kobayashi, K. *et al.* Distinct expression of TRPM8, TRPA1, and TRPV1 mRNAs in rat primary afferent neurons with aδ/c-fibers and colocalization with trk receptors. *J. Comp. Neurol.* **493,** 596–606 (2005).
27. Tominaga, M. *et al.* The cloned capsaicin receptor integrates multiple pain-producing stimuli. *Neuron* **21,** 531–543 (1998).
28. Bandell, M. *et al.* Noxious cold ion channel TRPA1 is activated by pungent compounds and bradykinin. *Neuron* **41,** 849–857 (2004).
29. Macpherson, L. J. *et al.* Noxious compounds activate TRPA1 ion channels through covalent modification of cysteines. *Nature* **445,** 541–545 (2007).
30. Hinman, A., Chuang, H. H., Bautista, D. M. & Julius, D. TRP channel activation by reversible covalent modification. *Proc. Natl Acad. Sci. USA* **103,** 19564–19568 (2006).
31. Prober, D. A. *et al.* Zebrafish TRPA1 channels are required for chemosensation but not for thermosensation or mechanosensory hair cell function. *J. Neurosci.* **28,** 10102–10110 (2008).
32. Hamada, F. N. *et al.* An internal thermal sensor controlling temperature preference in *Drosophila*. *Nature* **454,** 217–220 (2008).
33. Viswanath, V. *et al.* Opposite thermosensor in fruitfly and mouse. *Nature* **423,** 822–823 (2003).
34. Krochmal, A. R., Bakken, G. S. & LaDuc, T. J. Heat in evolution's kitchen: evolutionary perspectives on the functions and origin of the facial pit of pitvipers (Viperidae: Crotalinae). *J. Exp. Biol.* **207,** 4231–4238 (2004).
35. Safer, A. B. & Grace, M. S. Infrared imaging in vipers: differential responses of crotaline and viperine snakes to paired thermal targets. *Behav. Brain Res.* **154,** 55–61 (2004).
36. Kishida, R., Goris, R. C., Terashima, S. & Dubbeldam, J. L. A suspected infrared-recipient nucleus in the brainstem of the vampire bat, *Desmodus rotundus*. *Brain Res.* **322,** 351–355 (1984).
37. Jordt, S. E., McKemy, D. D. & Julius, D. Lessons from peppers and peppermint: the molecular logic of thermosensation. *Curr. Opin. Neurobiol.* **13,** 487–492 (2003).
38. Komatsu, H., Mori, I., Rhee, J. S., Akaike, N. & Ohshima, Y. Mutations in a cyclic nucleotide-gated channel lead to abnormal thermosensation and chemosensation in *C. elegans*. *Neuron* **17,** 707–718 (1996).
39. Ramot, D., MacInnis, B. L. & Goodman, M. B. Bidirectional temperature-sensing by a single thermosensory neuron in *C. elegans*. *Nature Neurosci.* **11,** 908–915 (2008).
40. Story, G. M. *et al.* ANKTM1, a TRP-like channel expressed in nociceptive neurons, is activated by cold temperatures. *Cell* **112,** 819–829 (2003).
41. Caspani, O. & Heppenstall, P. A. TRPA1 and cold transduction: an unresolved issue? *J. Gen. Physiol.* **133,** 245–249 (2009).
42. Wang, G. *et al. Anopheles gambiae* TRPA1 is a heat-activated channel expressed in thermosensitive sensilla of female antennae. *Eur. J. Neurosci.* **30,** 967–974 (2009).
43. Matsuura, H., Sokabe, T., Kohno, K., Tominaga, M. & Kadowaki, T. Evolutionary conservation and changes in insect TRP channels. *BMC Evol. Biol.* **9,** 228 (2009).
44. Dong, S. & Kumazawa, Y. Complete mitochondrial DNA sequences of six snakes: phylogenetic relationships and molecular evolution of genomic features. *J. Mol. Evol.* **61,** 1432 (2005).
45. Liman, E. R. Use it or lose it: molecular evolution of sensory signaling in primates. *Pflugers Arch.* **453,** 125–131 (2006).
46. Myers, B. R., Sigal, Y. M. & Julius, D. Evolution of thermal response properties in a cold-activated TRP channel. *PLoS One* **4,** e5741 (2009).
47. Chuang, H. H., Neuhausser, W. M. & Julius, D. The super-cooling agent icilin reveals a mechanism of coincidence detection by a temperature-sensitive TRP channel. *Neuron* **43,** 859–869 (2004).
48. DeCoursey, T. E. & Cherny, V. V. Temperature dependence of voltage-gated H^+ currents in human neutrophils, rat alveolar epithelial cells, and mammalian phagocytes. *J. Gen. Physiol.* **112,** 503–522 (1998).

Supplementary Information is linked to the online version of the paper at www.nature.com/nature.

Acknowledgements We thank A. Priel for advice and assistance with calcium imaging and electrophysiology, C. Chu for help with sequencing, J. Poblete for technical assistance, and the staff of the Natural Toxins Research Center serpentarium for animal husbandry. We thank P. Garrity for providing the d*TrpA1* cDNA. This work was supported by a Ruth L. Kirschstein National Research Service Award (GM080853) (N.T.I.), a NIH Institutional Research Service Award in Molecular and Cellular Basis of Cardiovascular Disease (A.T.C.), the Howard Hughes Medical Institute (J.S.W.), and grants from the National Institutes of Health, including NCRR Viper grant P40 RR018300-06 (E.E.S. and J.C.P.), P01 AG010770 (J.S.W.) and NS047723 and NS055299 (D.J.).

Author Contributions E.O.G., J.F.C.-M. and N.T.I. designed and performed experiments and analysed data. N.T.I. and J.S.W. developed analytical tools and analysed data. Y.M.K., G.H. and A.T.C. performed experiments and/or provided reagents and analysed data. E.E.S. and J.C.P. supervised snake husbandry and handling. E.O.G., Y.M.K., J.F.C.-M. and D.J. wrote the manuscript with discussion and contributions from all authors. J.S.W. and D.J. provided advice and guidance throughout. D.J. initiated and supervised the project.

Author Information Deep sequencing data are archived under GEO accession number GSE19911. GenBank accession numbers are GU562965 (*Python regius* TRPA1), GU562966 (*Elaphe obsoleta lindheimeri* TRPA1), GU562967 (*Crotalus atrox* TRPA1), GU562968 (*Crotalus atrox* TRPV1), and GU562969 (*Corallus hortulanus* TRPA1). Reprints and permissions information is available at www.nature.com/reprints. The authors declare no competing financial interests. Correspondence and requests for materials should be addressed to D.J. (julius@cmp.ucsf.edu or david.julius@ucsf.edu).

METHODS

Deep sequencing and analysis. Sequencing libraries were prepared from poly A^+ RNA using the Illumina mRNA-Seq Sample Prep Kit according to the manufacturer's instructions. Libraries were then sequenced on the Illumina Genome Analyser II using two 36-cycle sequencing kits to read 80 nucleotides of sequence from a single end of each insert, by standard protocols. Between 2.4 and 12.5 million inserts were sequenced for each sample.

Sequences were aligned to the chicken RefSeq protein database (NCBI version 2.1) using the blastx tool from NCBI blast (version 2.2.21), which aligns a six-frame translation of each query against a protein database. The alignment was performed with a word size of four amino acids and a window size of five; a maximum E value of 1×10^{-5} was required. For each read that aligned to the chicken proteome, a set of optimal hits was collected based on alignments whose bit score was within 0.2 of the highest bit score reported for that sequencing read. Each RefSeq alignment for a given sequencing read was converted to an Entrez Gene identifier and redundant alignments for a single read (which correspond to alignments against different isoforms of the same protein) were collapsed. The number of optimally aligning reads was then counted for each gene; in some cases a single read counted towards several genes. Multiple sequence alignment was performed with MUSCLE v3.70 and the tree was built from the MSA using PhyML 3.0. The multiple sequence alignment of all TRPA1 amino acid sequences was constructed using MUSCLE (version 3.70) using the default parameters. The unrooted phylogenetic tree was constructed from this multiple sequence alignment using PhyML (version 3.0) with default parameters and maximum likelihood estimation of the gamma shape parameter and the fraction of invariant sites. Bootstrapping was performed with 100 trials.

***In situ* hybridization histochemistry.** Adult snakes were euthanized with beuthanasia-D (1 ml per 4.5 kg body weight). TG and DRG tissue were dissected and fixed in 4% paraformaldehyde in PBS for 5 days. Cryostat sections (12–15-μm thick) were processed and probed with a digoxigenin-labelled cRNA. Probes were generated by T7/T3 *in vitro* transcription reactions using a 2.9-kb fragment of *TRPA1* cDNA (nucleotides 153–3024) and 1.9-kb fragment of *TRPV1* cDNA (nucleotides 417–2387). Signal was developed with alkaline phosphatase-conjugated anti-digoxigenin Fab fragments according to the manufacturer's instructions.

Channel cloning. Functional cDNAs were amplified from single-stranded DNA, generated by reverse transcriptase reaction, using the following primers: rattlesnake *TRPA1*, non-pit *TRPA1* and royal python *TRPA1* (forward: 5′-GAAT GACCAGGAGCTGTATC-3′; reverse: 5′-AGCCAGCTTGACTGGAATTG-3′); rattlesnake *TRPV1* (forward: 5′-CAGGTGAGGTGAGTCCTTCGTAAC-3′; reverse: 5′-TGAATGACGCAGATGGGGGTC-3′).

Calcium imaging. All tested channels were transiently expressed in HEK293 cells with the use of Lipofectamin 2000 (Invitrogen), and cells were maintained in medium containing ruthenium red (3 μM). Calcium imaging of HEK293 cells using Fura-2/AM was performed on coverslips coated with Matrigel (BD). Fluorescent images were acquired with Metaflour software (Molecular Device) and analysed using Graph Pad Prism 4.

Culture of sensory neurons. Snake were anaesthetized using isofluorane and then decapitated. TGs were isolated and cultured as previously described[17]. In brief, dissected ganglia were first placed in ice-cold DMEM/F12 solution. Cells were dissociated from trigeminal ganglia by treatment with collagenase (1 mg ml^{-1}, 50 min, 28 °C) and trypsin (10 min, room temperature) followed by mechanical dissociation with plastic pipette. Dissociated cells were centrifuged at 1,000*g* for 10 min and then diluted with DMEM/F12, 10% FBS, penicillin/streptomycin and 2 mM glutamine. Cells were plated onto the Matrigel-precoated coverslips. Cells were maintained at 28 °C in 7% CO_2, 93% air for 6–48 h.

Oocyte electrophysiology. Surgically extracted oocytes from *Xenopus laevis* (Nasco) were cultured and analysed 2–5 days after injection by TEVC as previously described[47]. Oocytes were injected with 5 ng RNA and whole-cell currents measured after 24–72 h using a Geneclamp 500 amplifier (Axon Instruments, Inc.). Microelectrodes were pulled from borosilicate glass capillary tubes to obtain resistances of 0.3–0.07 MΩ. Bath solution contained 10 mM HEPES, 120 mM NaCl, 2 mM KCl, 0.2 mM EGTA, 1 mM $CaCl_2$ and 2 mM $MgCl_2$ buffered to a final pH of 7.4 with NaOH. Data were analysed using pCLAMP10 software.

Patch-clamp recording. Membrane currents were recorded using gap free protocol at −60 mV under the whole-cell configuration of the patch-clamp technique using Axopatch 200B amplifier (Axon Instruments). Membrane currents were digitized online using a Digidata 1440A interface board and pCLAMP 10.2 software (Axon Instruments). Sampling frequency was set to 5 kHz, and the low-pass filter was set to 1 kHz. Patch electrodes were fabricated from borosilicate glass with a resistance of 2–4 MΩ. The bath solution contained (mM): 130 NaCl, 3 KCl, 1.2 $MgSO_4$, 2 $CaCl_2$, 10 HEPES, 10 glucose, adjusted to pH 7.4. The perfusion solution was the same as the bath solution but with 0.2 mM $CaCl_2$ to reduce the desensitization process. The pipette solution contained (mM): 130 $CsMeSO_4$, 20 CsCl, 9 NaCl, 0.2 EGTA, 10 HEPES, 1 MgATP, and adjusted to pH 7.2. Thermal stimulation was applied with a custom-made Peltier device (Reid-Dan Electronics) that heated or cooled the flowing perfusate stream. Temperature was measured using a thermistor placed adjacent to the cell.

Determination of thermal threshold. Temperature thresholds represent the point of intersection between linear fits to baseline and the steepest component of the Arrhenius profile. Values are derived from averages of individual curves; $n \geq 6$. Arrhenius curve were obtained by plotting the current on a log-scale against the reciprocal of the absolute temperature. Q_{10} was used to characterize the temperature dependence of the ionic current as calculated using the following equation:

$$Q_{10} = \left[\frac{R_2}{R_1}\right]^{10/(T_2 - T_1)}$$

where R_2 is the current at the higher temperature T_2, and R_1 is the current at the lower temperature T_1 (ref 48).